ELSEVIER

Journal of Molecular Catalysis A: Chemical 139 (1999) 31–41

JOURNAL OF MOLECULAR CATALYSIS A: CHEMICAL

Pathway of the cycle between the oxidative adsorption of SO_2 and the reductive decomposition of sulfate on the $MgAl_{2-x}Fe_xO_4$ catalyst

Jin-an Wang [a,*], Ze-lin Zhu [b], Cheng-lie Li [b]

[a] *Institute of Physics, National University of Mexico (UNAM), P.O. Box 20-364, 01000 Mexico DF, Mexico*
[b] *Petroleum Processing Research Center, East China University of Science and Technology, Shanghai 200237, China*

Received 24 October 1997; accepted 30 April 1998

Abstract

The behaviors of the SO_2 oxidative adsorption and the reduction decomposition of formed sulfate over Mg–Fe–Al–O mixed spinel catalyst were studied by in situ IR, MR–GC–MS, Mössbauer spectroscopy and electrical conductivity measurement techniques. In the oxidative adsorption and/or reaction process, SO_2 and oxygen molecules are adsorbed on the lattice oxygen ions and oxygen vacancies, respectively. During the SO_2 adsorption and reaction, adsorbed sulfur species react with the lattice oxygen ions and form the sulfite-like species. When oxygen molecules are present in the feed mixture, sulfate is formed from the sulfite-like species reacting with the adsorbed oxygen ions. When the sulfated samples are reduced by hydrogen at 773 K, a large amount of H_2S along with a small part of SO_2 is produced. Different iron species, Fe^{3+}, $Fe^{2.5+}$, Fe^{2+} and Fe^0 are identified in the sulfated sample during the reduction process. In the half cycle of SO_2 oxidative adsorption and reaction, iron ions are directly involved in the formation of the mixed sulfate; in the half cycle of the reduction, due to the S–O–Fe bond being easily broken, the reducibility of the mixed sulfate hence is improved. A mechanism on the cycle between SO_2 oxidative adsorption and sulfate reductive decomposition is proposed.

Keywords: Sulfur-transfer catalyst; Mg–Fe–Al–O; De-SO_2; Pollution control; Mechanism

1. Introduction

Sulfur dioxide is an atmospheric pollutant, which can lead to the formation of the sulfur-type acid rain [1–3]. In the fluid catalytic cracking units (FCCU), 45–55% of the organic sulfur in the feed stock is converted to H_2S in the stripper and reactor; 35–45% of them remain as part of the liquid products and about 5% is deposited on the coke existing on the surfaces of the FCC catalysts. During the coke containing the sulfur compound is burned off in the regenerator, SO_x (about 90% SO_2 and 10% SO_3) emissions are produced [4–6].

* Corresponding author. Tel.: +52-5-6225129; Fax: +52-5-6161535; E-mail: wang_ja@fenix.ifisicacu.unam.mx

1381-1169/99/$ - see front matter
PII: S1381-1169(98)00186-1

Lowell et al. [7], evaluated 47 different metal oxides for choosing the absorbents of dioxide sulfur. A group of 16 oxides, including the oxides of aluminum, magnesium and cerium, were found useful for SO_2 control. The evaluation, however, was only based on the thermal regeneration of the absorbents and the regeneration under reduction conditions was not considered.

Aluminum oxide was often used as an additive to remove the SO_x emissions. However, in the operation conditions of the FCC process, the $Al_2(SO_4)_3$ formed by the SO_2 adsorption and reaction with alumina, is not stable. For example, the operation temperature in the regenerator of FCC is as high as 973 K, in such case, the $Al_2(SO_4)_3$ readily decomposes and releases SO_2. Hence, the efficiency of SO_2 adsorption on alumina is reduced [8].

On the other hand, it has been proved that MgO has a higher De-SO_x activity than that of Al_2O_3. Unfortunately, the reducibility of the $MgSO_4$ formed is very low in the FCC operation conditions. This results in a loss of its activity. In addition, the attrition resistance of MgO is very poor compared to that of the FCC catalysts [9]. Nevertheless, owing to these shortcomings, MgO can not be considered as a commercial De-SO_x catalyst.

Ruthenium, rhodium, palladium and platinum can be used as active promoters to enhance the ability of the SO_x-absorbents in the regeneration zone of the FCC unit. However, these absorbents can also promote the formation of nitrogen oxides in the regenerator [10]. Nitrogen oxides are another kind of atmospheric pollutant that should be controlled. Moreover, the cost of the precious metals is very expensive. Therefore, precious metals are rarely used as promoters for the SO_x control in the FCC process.

Recently, more attention has been paid to a so-called sulfur-transfer catalyst that is used as an additive to mix with the FCC catalyst for SO_x reduction. Magnesium–alumina spinel materials have been proven to be a good kind of sulfur-transfer catalysts because they have not only a better adsorbing SO_x activity but also a higher thermal stability in comparison with Al_2O_3 and MgO [8,11].

For the De-SO_2 catalyst, the reducibility of the sulfate formed by the adsorbed SO_2 reacting with the metal active component of the catalyst determines the lifetime of the catalyst. If the sulfate cannot be removed from the active sites on the catalyst during the cracking reaction process in the reactor and stripper, the catalyst will lose its activity. Therefore, the reducibility of the sulfate is the essential factor for choosing a high quality sulfur-transfer catalyst in the industrial application. Although the magnesium–alumina spinel catalyst has the higher ability of SO_2 adsorption activity compared with MgO or Al_2O_3, however, the reducibility of the sulfate on this catalyst is relatively limited.

It has been reported that when the Al^{3+} ion is partially substituted by Fe^{3+} in the structure of the magnesium–alumina spinel, both the SO_2 adsorption activity and the reducibility of the sulfate are improved [12–14]. Other transition metal ions, for instance, vanadium and copper, have the functions similar to that of the iron ion when they are introduced into the magnesium–alumina spinel structure [15,16].

Although some De-SO_x catalysts have been used in the FCC units for some years, the mechanism of SO_2 adsorption on the catalyst surface is not clear. The pathways of the cycle between the SO_2 oxidative adsorption and the sulfate reductive decomposition have not been reported yet, even if such mechanisms are very important for developing new De-SO_2 catalysts.

In the present work, Mg–Al–Fe–O mixed spinel catalyst was prepared by the coprecipitation method. The adsorption of SO_2 and O_2 on the catalyst was studied by the electrical conductivity measurement techniques. In the cases of SO_2 adsorption and oxidative adsorption, the different sulfur species were characterized by in situ IR technique. The roles of the iron ions and a pathway of the cycle between the SO_2 oxidative adsorption and the sulfate reductive decomposition are reported.

2. Experimental

2.1. Catalyst preparation

The $MgAl_{2-x}Fe_xO_4$ ($x = 0.2$) catalyst was prepared by the coprecipitation method. The precursor materials were magnesium nitrate, sodium aluminate and ferric nitrate. Three different solutions were respectively prepared by adding 51.80 g $Mg(NO_3)_2 \cdot 6H_2O$, 16.48 g $Fe(NO_3)_3 \cdot 9H_2O$ and 40.80 g $NaAlO_2$, respectively into three different containers, each holding 300 ml of deionized water. At a same rate, these solutions were added into a 2000-ml container, which contains 500 ml of deionized water. During the addition, the formed slurry was stirred and the pH value was controlled at 8–9 using the concentrated nitric acid solution or 2N NaOH solution. Afterwards, the slurry was continuously stirred for 1 h and then aged at room temperature over night. The aged slurry was filtered and washed with deionized water. The filtered cake was dried at 393 K for 10 h and then calcined at 1073 K for 4 h in a furnace. The product was ground and 80–160 mesh powders were used in the experiments.

2.2. In situ IR characterization

The in situ IR measurements were carried out on a HITACHI-270-30 IR spectrometer under the vacuum conditions and at different adsorption temperatures from 323 to 823 K. The adsorption cell is an H-type quartz tube with KBr windows. This adsorption–desorption system is on line with a vacuum set, which is combined with two mechanic pumps and a two-stage oil diffuse pump. Before the adsorption operation, the sample was heated in the adsorption cell for 2 h at 573 K with the evacuation. In the case of SO_2 adsorption, 500 Torr of SO_2 were introduced into the IR adsorption system. In the case of the SO_2 oxidative adsorption, a mixture of 500 Torr of SO_2 and 100 Torr of O_2 was fed.

2.3. Electrical conductivity measurements

The conductivity of the catalyst was determined on an ECTA system equipped with a vacuum system. This experimental system can work under different temperatures and various gaseous atmospheres. Four Pt-electrodes connected to the surface of the samples. Prior to measurement, the sample was evacuated at 673 K for 2 h under a 0.5 Pa pressure, to remove the impurities adsorbed on the catalyst surface. Then a flow of SO_2 or O_2 was introduced into the adsorption cell at 773 K. Partial pressures of SO_2 and O_2 were controlled from 50 Torr to 200 Torr according to the experimental requirements. The electrical conductivity of the sample was calculated using the following equation:

$$\sigma = 1/\rho = (1/R) \times (L/S), \quad (1)$$

where σ is the electrical conductivity, ρ is the resistivity, R is the electrical resistance and L/S is the geometric factor (L is the thickness of the sample and S the section area of the electrodes).

2.4. Mössbauer spectroscopy

The Mössbauer spectra were recorded at room temperature on an AME-50 spectrometer with ^{57}Co in palladium base as the radioactive source. The samples were pretreated at different conditions. All the spectra were computer fitted assuming Lorentzian line shapes. The Debye–Waller factors were used to correct the data. The isomer shifts and the velocities relative to the α-Fe foil standard are reported.

2.5. Catalytic test

Tests for the reducibility of the sulfate formed in the catalysts were performed on the MR–GC–MS system. The reactor was a 1.5-cm o.d. quartz tube which was placed in a single-zone furnace controlled by a YCC-16 temperature-programmed controlling system. Two thermo-

couples were positioned just below the top of the catalyst bed to measure the temperatures.

In the adsorption or oxidative adsorption process, 90 mg De-SO_2 catalyst mixed with 3 g FCC Catalyst (supplied by China Jinling Petrochemical Cooperation) was heated at 973 K under a flow of N_2 for 20 min. Then 5% O_2 in N_2 was introduced into the reactor for 5 min. Afterwards, a gaseous mixture containing 1.5% SO_2, 5% O_2 in N_2 was fed for 20 min at 973 K.

In the reduction half cycle, the temperature was 773 K; 30% H_2 in nitrogen was used as the reduction gas. The desorbed species or the reductive products were determined in a mass spectrometer that is on line with the reaction set. During the reduction process, every 3 min of reduction, 0.5 ml of the outlet gases were injected into the MS apparatus for analyzing the concentration of each component. The experimental conditions were close to the actual conditions used in the FCC process. The operation temperature in the regenerator where SO_2 is captured by the catalysts in the oxidative atmosphere is 973 K; the temperature in the reactor where sulfate is reduced to H_2S is 773 K.

3. Results and discussion

3.1. Adsorption sites of oxygen and SO_2

The results of the electrical conductivity measurements when SO_2 is adsorbed on the $MgAl_{1.8}Fe_{0.2}O_4$ catalyst are summarized in Table 1. It is found that the electrical conductivity increases as the partial pressure of SO_2 increases. For example, in the first 5 min, the electrical conductivity ($\log \sigma$) increases from -5.30 to -5.02, -4.21 and -4.02 $(\Omega\ \mathrm{cm})^{-1}$ when the pressure of SO_2 increases from 50 to 100, 150 and 200 Torr, respectively. These results suggest that the conduction electrons are generated during SO_2 adsorption.

Although the influencing factors for electrical conductivity in oxide powders are complex, the variations of the electrical concentration as a function of experimental parameters, however, can be used to speculate the gas adsorption or reaction sites on the catalysts.

Table 1
Conductivity data ($-\log \sigma/(\Omega\ \mathrm{cm})^{-1}$) of SO_2 adsorption on $MgAl_{1.8}Fe_{0.2}O_4$ catalyst

Time (min)	SO_2 pressure (Torr)			
	200	150	100	50
5	4.02	4.21	5.02	5.30
10	3.60	4.10	4.83	5.04
20	3.05	3.76	4.45	4.87
30	2.56	3.15	4.02	4.66
40	2.33	3.02	3.70	4.43
50	2.05	2.87	3.56	4.33
60	1.94	2.73	3.31	4.26

In general, metal ions (M^{n+}), lattice oxygen O_L^{2-} and oxygen vacancies (V_o) coexist in the surface of the catalyst. After evacuating at 773 K, more oxygen vacancies should be created in the surface and bulk of the catalyst. Two free-like electrons are located at each V_o according to Eq. (2):

$$O_L^{2-} \rightleftharpoons 1/2O_2(g) + V_o^{\cdot\cdot}, \quad (2)$$

where $V_o^{\cdot\cdot}$ stands for an oxygen vacancy with two electrons. Assuming that one SO_2 molecule is adsorbed on an oxygen vacancy, the conductivity should decrease as the SO_2 partial pressure increases, because the adsorption of SO_2 on oxygen vacancies consumes the conduction electrons trapped at oxygen vacancies, resulting in a diminishing of the conduction electron concentration. Obviously, this assumption is inconsistent with the measurement results.

On the other hand, if one SO_2 molecule adsorbs on the lattice oxygen in the $MgAl_{1.8}Fe_{0.2}O_4$ catalyst, according to the following equilibrium:

$$SO_2(g) + O^{2-}(\text{lattice}) \rightleftharpoons SO_3^-(\text{ads}) + e^-, \quad (3)$$

an electron can be released from the lattice oxygen ion. Increasing the SO_2 pressure, the equilibrium (3) will shift to the right, increasing the concentration of the conduction electron. In this case, the electrical conductivity will be increased. The results of SO_2 adsorption are in

Table 2
Conductivity data ($-\log \sigma/(\Omega\ \mathrm{m})^{-1}$) of O_2 adsorption on $MgAl_{1.8}Fe_{0.2}O_4$ catalyst

Time (min)	O_2 pressure (Torr)			
	200	150	100	50
5	5.62	5.90	5.54	5.20
10	6.50	6.37	5.93	5.56
20	6.62	6.45	6.27	5.75
30	6.64	6.47	6.33	5.84
40	6.66	6.48	6.35	5.90
50	6.67	6.48	6.37	5.94
60	6.67	6.48	6.38	5.95

agreement with the second assumption, therefore, we deduce that the lattice oxygen ions in the $MgAl_{1.8}Fe_{0.2}O_4$ catalyst appear as the adsorption sites of SO_2.

The data presented in Table 1 and the equilibrium (3) clearly show that during the SO_2 adsorption, adsorbed SO_2 molecules react with the lattice oxygen ions and form the sulfur species SO_3^-. In particular, the release of the electron from the oxygen vacancy is determined by the reaction. These results indicate that the SO_2 adsorption is the process accompanying by the chemical reaction. Therefore, in the study of the electrical conductivity as function of the adsorption time, both possibilities, the SO_2 adsorption and reaction with the active sites, should be considered.

The results of conductivity measurements shown in Table 2 show that the oxygen vacancies are the possible sites for O_2 adsorption. This assumption is supported by the fact that during the oxygen adsorption, the electrical conductivity decreases as the oxygen partial pressure increases. This result is in good accordance with the following equations:

$$1/2O_2(g) + V_o^{\cdot\cdot} \rightleftharpoons O^-(ads) + V_o^{\cdot}, \quad (4)$$

$$O^-(ads) + V_o^{\cdot} \rightleftharpoons O_L^{2-}(ads). \quad (5)$$

When an oxygen molecule adsorbs on an oxygen vacancy, the electrons trapped in this site are captured by the molecular oxygen forming adsorbed oxygen ions and hence a reduction of the electrical conductivity is observed.

From the data shown in Tables 1 and 2, it is also found that the adsorption (or reaction) rates of oxygen and SO_2 are relatively rapid in the initial period (10 min). This is likely due to the high concentration of the active sites on the fresh sample. Furthermore, it seems that the adsorption of O_2 on the oxygen vacancies is easier than the SO_2 adsorption and reaction on lattice oxygen sites according to that after 20 min of oxygen adsorption, the conductivity remains almost unchanged. This shows that the Eqs. (4) and (5) reach their equilibrium. However, in the case of SO_2 adsorption and reaction, after 60 min, the electrical conductivity still slowly increased.

3.2. In situ IR characterization of SO_2 adsorption and oxidative adsorption

To identify the surface species during the adsorption of SO_2 and/or O_2, in situ IR measurements were carried out. In the absence of oxygen in the feed gas, the SO_2 adsorbed on the catalyst, three IR absorption bands respectively located at 850, 910 and 1340 cm^{-1} were observed (Fig. 1). On the evacuation at 373 K, the

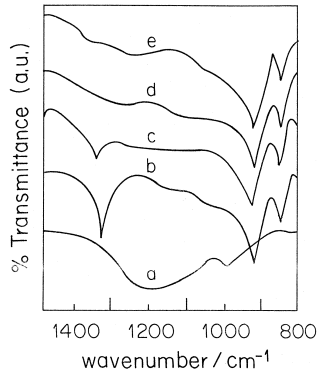

Fig. 1. In situ IR spectra of SO_2 adsorption on the $MgAl_{2-x}Fe_xO_4$ ($x = 0.2$) catalyst. (a) Sample evacuated at 673 K. (b) SO_2 adsorption at 477 K for 1 h. (c) After SO_2 adsorption at 477 K for 1 h, the sample was evacuated at 477 K for 0.5 h. (d) After SO_2 adsorption at 477 K for 1 h, the sample was evacuated at 673 K for 0.5 h. (e) After SO_2 adsorption at 577 K for 1 h, the sample was evacuated at 673 K.

band at 1340 cm^{-1} rapidly disappeared, and hence, this signal was assigned to the physically adsorbed species. The bands at 850 and 910 cm^{-1} had only a little reduction after evacuating at 673 K for 0.5 h. They were ascribed to the surface sulfite-like complexes. Baldwin [17], reported that for free SO_3^{2-} ion, the symmetric and asymmetric stretching frequencies of S–O band show two absorption peaks at 1010 cm^{-1} and 961 cm^{-1}, respectively. SO_3^{2-} bonded to a metal atom by its sulfur atom (M–S–O), its symmetry, C_{v3}, remains unchanged. On the other hand, if the coordination to a metal atom is given through the oxygen atom, the asymmetric stretching frequency splits into two bands: 902 cm^{-1} and 862 cm^{-1}. We hence propose here that in the case of SO_2 adsorption and reaction, sulfite-like species (SO_3^-).

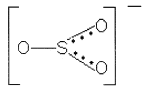

is formed by SO_2 reacting with the lattice oxygen ions. This suggestion is also in agreement with the results of the electrical conductivity measurements (Scheme 1 and Eq. (3)).

When oxygen is contained in the feed mixture, the in situ IR spectra obtained are shown in Fig. 2. Four bands respectively located at 910, 1070, 1200 and 1400 cm^{-1} were observed. After evacuating at 673 K for 1 h, these bands did not show appreciable reduction. IR spectra suggest that these bands characterize the stable sulfur complexes resulting from the SO_2 strong chemisorption or reaction with the active sites.

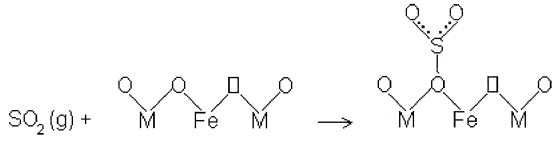

Scheme 1. SO_2 adsorbed on the lattice oxygen sites of the catalyst then reacts with this lattice oxygen ion to form sulfite-like species. (□) Stands for an oxygen vacancy; (M) stands for Al^{3+} or Mg^{2+} ion.

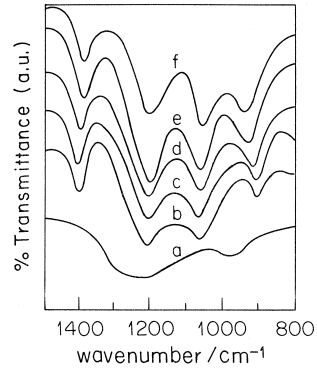

Fig. 2. In situ IR spectra of SO_2 oxidative adsorption on the $MgAl_{2-x}Fe_xO_4$ ($x = 0.2$) catalyst. (a) Sample evacuated at 673 K. (b) SO_2 oxidative adsorption at 573 K for 0.5 h. (c) SO_2 oxidative adsorption at 673 K for 0.5 h. (d) SO_2 oxidative adsorption at 773 K for 0.5 h. (e) SO_2 oxidative adsorption at 773 K for 2 h. (f) SO_2 oxidative adsorption at 673 K for 0.5 h, and then evacuation for 0.5 h.

When SO_4^{2-} coordinates to two metal ions through two of its oxygen atoms, a chelating or a bridged bidentate complex is formed. Mateus and Fresco [18], assigned the adsorption bands at 1195–1160 (ν_3), 1110–1105 (ν_3), 1035–1030 (ν_3) and 990–960 cm^{-1} (ν_1) to the asymmetric and symmetric stretching frequencies of the double-like S⩲O band and S–O band in the structure of bridge complex. Obviously, IR results in this work differ from theirs, because the band at 1400 cm^{-1} was observed in this work. Our results are similar to that observed in the sulfuric acid molecule. Sulfuric acid molecule shows adsorption bands at 1440–1350, 1230–1150, 1000–960 and 910 cm^{-1}, which are attributed to the C_v point group [19,20]. In the present work, the bands at 1400 and 1200 cm^{-1} are also assigned to the asymmetric stretching frequencies and symmetric stretching frequencies (ν_{as} and ν_a) in the SO_4^{2-} ion.

Because the sulfate is formed only in the case of oxygen presented in the fed stream, the adsorbed oxygen, therefore, have an important role in the formation of sulfate. Probably, the sulfate ion (SO_4^{2-}) is produced from the adsorbed oxygen species (O^-) reacting with sulfite-like species SO_3^- (Scheme 2).

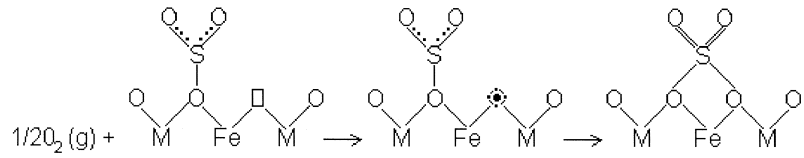

Scheme 2. Sulfate is formed during the SO_2 oxidation adsorption and reaction procedure. (solid circle inside a dotted circle) Stands for an adsorbed oxygen species; (M) stands for Al^{3+} or Mg^{2+} ion.

3.3. Sulfate reductive decomposition

The results for the isothermal reduction by H_2 in the sulfated samples are shown in Figs. 3 and 4. It was found that during the first 5 min of the reduction at 773 K, a large amount of H_2S with a small amount of SO_2 was produced. When the sulfating temperature increased from 773 K to 973 K, and then reduced by H_2 at 773 K, the concentration of SO_2 in the products decreased from 6% to 1%.

These results significantly differ from those reported by Nam and Gavalas [21,22]. In their paper, the SO_2 desorption is dominant and H_2S occurs in a smaller amount. It is noted that SO_2 is often yielded in the beginning of the reduction procedure. Because before the reduction, the sulfated sample was treated in a He stream at the same temperature for half an hour, the physically adsorbed SO_2 should be desorbed in this procedure. Therefore, the physically adsorbed SO_2 is not responsible for the observed SO_2.

The amount of SO_2 is likely related to the different modes of chemisorption SO_2. Studies of the basic properties show that both the weak and strong basic centers coexist in the surface of the $MgAl_{2-x}Fe_xO_4$ catalysts and the concentration of the weak basic center is low [23]. SO_2 is a strong acid gas, its adsorption and reactivity are affected by the basicity of the catalyst. Some adsorbed SO_2 on the weak basic sites in weakly chemical bonds were stable in the pretreatment, but they easily desorb or decompose during the reduction. Because the concentration of the weak basic centers is low, the sites for

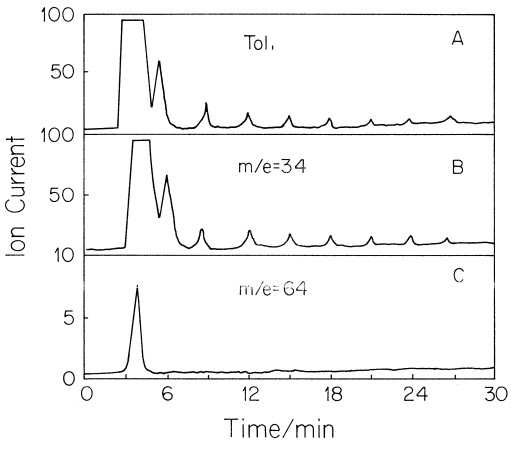

Fig. 3. Ion current as a function of reaction time at 773 K. The sample firstly was treated at 973 K for 30 min using the mixture of 1.2 vol% SO_2 and 20 vol% O_2 in N_2. Then the sample was reduced using 30 vol% H_2 at 773 K. The concentration of each component in the outlet stream during the reaction was analyzed by the MR–GC–MS system. Every 3 min about 0.5 ml outlet gas was injected into the measurement system for analysis. (A) Total ion current; (B) ion current of $m/e = 34$ which corresponds to H_2S; (C) ion current of $m/e = 64$ which corresponds to SO_2.

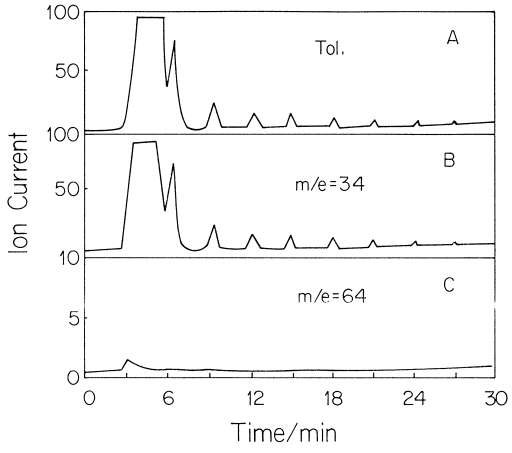

Fig. 4. Ion current as a function of reaction time at 773 K. The sample firstly was treated at 773 K for 30 min using the mixture of 1.2 vol% SO_2 and 20 vol% O_2 in N_2. Then the sample was reduced using 30 vol% H_2 at 773 K. The concentration of each component in the outlet stream during the reaction was analyzed by the MR–GC–MS system. Every 3 min about 0.5 ml outlet gas was injected into the measurement system for analysis. (A) Total ion current; (B) ion current of $m/e = 34$ corresponds to H_2S; (C) ion current of $m/e = 64$ corresponds to SO_2.

SO_2 adsorption in a weakly chemical mode are limited. Therefore, the amount of SO_2 in the products was less that 6%. These results agree well with the electrical conductivity results where the lattice oxygen ions are suggested as SO_2 adsorption or reaction centers. The lattice oxygen is often believed as the basic centers due to that it is an electron-rich site. Increasing the adsorption temperature would result in a decrease of SO_2 molecules adsorbed on the weak sites. Hence, during the reduction process, less SO_2 was yielded when the sample was sulfated at 973 K than at 773 K.

During the reduction process, probably H_2 first attacked the S–O–Fe bond and captured the oxygen ion. This results in the breaking of the bond between Fe and sulfur ion, leaving one oxygen vacancy and reduced iron species. Afterwards, the electron density around the sulfur ion group would be redistributed. In this process, the sulfur–oxygen ion group was very unstable. The continuing reduction by hydrogen would produce a large amount of H_2S.

3.4. Iron ion valences and coordinated environment

The Mössbauer spectroscopy was also used to analyze the chemical valences and the coordinate environments of the iron ions during the oxidation or reduction process (Fig. 5). Table 3 summarizes all the data of Mössbauer parameters.

Fig. 5A shows a double line. It is a typical line of high-spin Fe^{3+} ions in octahedral position, which indicates that in the case of SO_2 oxidation adsorption, all the iron ions are in Fe^{3+} oxidized state.

When the sample was first treated with the mixture of SO_2 and O_2 at 973 K for 20 min, and then reduced using hydrogen at 773 K for 20 min, it shows a complex Mössbauer spectra (Fig. 5B). The central doublet 1 is due to Fe^{3+} in a superparamagnetic state [24]. While, the doublet 2 was assigned to Fe^{2+} ion in coordinated tetrahedral sites in $FeAl_2O_4$ [25]. The

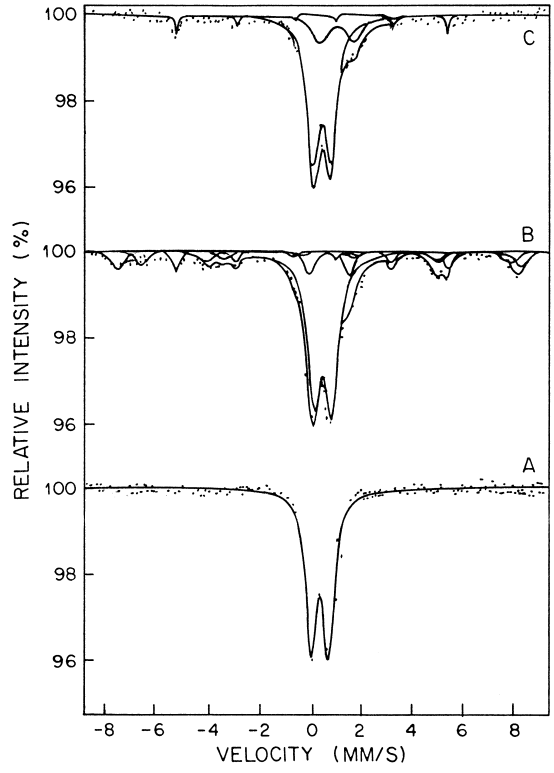

Fig. 5. Mössbauer spectra of the samples treated at different conditions. (A) The sample was treated using the mixture of 1.2 vol% SO_2 and 20 vol% O_2 in N_2 at 973 K for 30 min. (B) The sample was first treated using the mixture of 1.2 vol% SO_2 and 20 vol% O_2 in N_2 at 973 K for 30 min; then it was reduced using 30 vol% H_2 at 773 K for 20 min. (C) The fresh sample was reduced using 30 vol% H_2 at 773 K for 20 min.

existence of $FeAl_2O_4$ was also identified by XRD analysis [26]. The different sextet absorption lines imply that iron ions have different coordinate environments and that some iron ions in a high valence oxidized state are reduced to a lower valence state. Sextet 1 originates from Fe^{3+} ions occupying tetrahedral sites. Sextet 2 is characteristic of $Fe^{2.5+}$ ions, which is a consequence of the existence of Fe_3O_4. In Fe_3O_4, Fe^{3+} and Fe^{2+} ions in the octahedral environment cannot be distinguished for the fast electron hopping above the Verway temperature [27]. Here, the broadening of the absorption line suggests that Fe_3O_4 seems to be in a nonstoichiometric state. During the reduction process, the reduction of lattice oxygen leads to the occurrence of oxygen deficit. Hence, magnetite

Table 3
Parameters of the Mössbauer spectra of the samples treated at different conditions

Sample	Pretreatment	Spectra	Parameters			Area (%)	Assignments
			IS (mm/s)	QS (mm/s)	H (kOe)		
A	Sulfation at 973 K for 30 min	doublet	0.29	0.70		100	Fe^{3+}(B)
B	Sulfation at 973 K for 30 min and then reduced using H_2 at 773 K for 20 min	doublet 1	0.36	0.71		62.3	Fe^{3+}(B)
		doublet 2	0.59	1.64		7.6	Fe^{2+}(A)
		sextet 1	0.35	0.09	486.49	12.8	Fe^{3+}(A)
		sextet 2	0.65	0.06	449.69	10.0	$Fe^{2.5+}$(B)
		sextet 3	0.02	0.03	327.60	7.2	α-Fe^{o}
C	Unsulfated sample reduced using H_2 at 773 K for 20 min	doublet 1 doublet	0.28	0.72		74.8	Fe^{3+}(B)
		doublet 2	0.87	1.44		19.8	Fe^{2+}(A)
		sextet	0.04	0.08	328.5	5.4	α-Fe^{o}

with oxygen deficits can be described as $Fe_A^{3+}[Fe_x^{2+}Fe_y^{3+}]_BO_{4-\square}$ ($\square$ denotes vacancies) [28]. The existence of 7.2% α-Fe phase is responsible for sextets 3 [29]. From the above analysis, different iron species, Fe^{3+}, $Fe^{2.5+}$, Fe^{2+} and α-Fe^0, were identified after the sulfating sample was reduced by hydrogen.

When the sample is reduced by hydrogen at 500°C for 30 min without SO_2 adsorption pretreatment, the Mössbauer spectra are shown in Fig. 5C. Similar to the assignments in Fig. 5B, the doublet 1 line is ascribed to the octahedral Fe^{3+}; the doublet 2 is due to the Fe^{2+} ions in tetrahedral sites and the sextet line is the characterization of α-Fe^0.

When comparing the Mössbauer spectra of Fig. 5B and 5C, a significant difference is observed: Fe_3O_4 phase was not found in the unsulfated sample. As discussed above, lattice oxygen ions are the adsorption sites of oxygen, adsorbed oxygen ions react with adsorbed sulfite-like species and form the sulfate. Therefore, Fe_3O_4 phase with oxygen deficit appears to be an active species during SO_2 oxidation adsorption in the reduced sulfated sample.

3.5. Mechanism of SO_2 oxidative adsorption and sulfate reduction decomposition

The plausible mechanism for the cycle between the SO_2 oxidative adsorption and the sulfate reductive decomposition is proposed in Scheme 3. In the half cycle of the SO_2 oxidative adsorption or reaction, oxygen and SO_2 molecules respectively adsorb on the oxygen vacancy and lattice oxygen, producing adsorbed oxygen species (O^-) and sulfite-like ions (SO_3^-). Afterwards, the adsorbed oxygen species react with the SO_3^- ion forming sulfate ions (SO_4^{2-}). In the half cycle of reductive decomposition, a large amount of H_2S along with SO_2 is produced due to the reaction of the oxygen ions connecting the sulfur and iron ions in S–O–Fe bond with the hydrogen molecule, resulting in some reduced iron species and additional oxygen vacancies. The reduced iron species will be oxidized and the oxygen vacancies will be filled by oxygen in the following half cycle of the oxidative adsorption.

Here, it is worth noting that we suggest two different metal ions involving the formation of sulfate. This idea is supported by the fact that the thermal stability and the reducibility of sulfates are significantly affected by the metal ions. If only the magnesium ion is involved in the formation of sulfate to yield the $MgSO_4$, since the temperature corresponding to the maximum reduction rate of $MgSO_4$ is as high as 1173 K [30], in the operation condition of FCC process, the reductive decomposition of $MgSO_4$ is not pronounced. Obviously, this is not in agreement with the results of our reduction experiments, because almost the formed sulfates

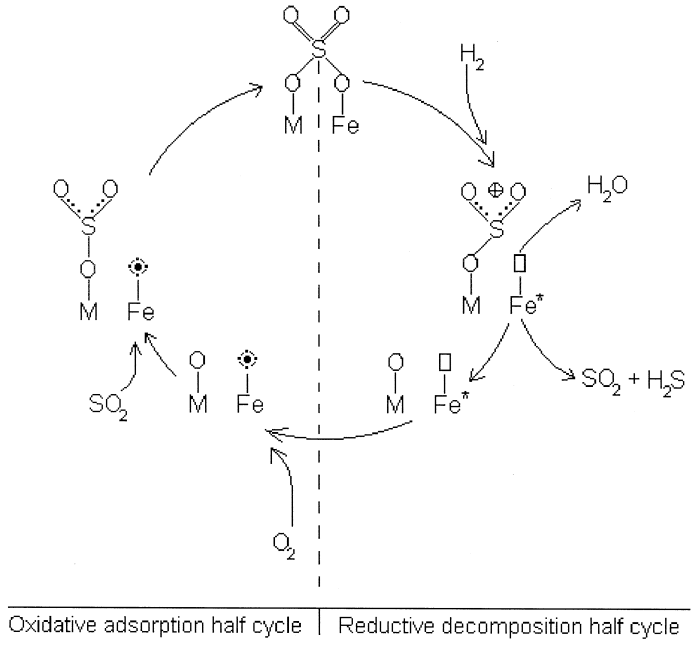

Scheme 3. Mechanism of SO_2 oxidative adsorption and sulfate reductive decomposition on the $MgAl_{2-x}Fe_xO_4$ ($x = 0.2$) catalyst. (M) Mg^{2+} or Al^{3+} ion; (Fe^*) reduced iron ion; (solid circle inside a dotted circle) adsorbed oxygen ion; (□) oxygen vacancy.

in this catalyst are removed in the reductive half cycle [31]. If only iron or aluminum ion contributes to the formation of the sulfate, $Al_2(SO_4)_3$ or $Fe_2(SO_4)_3$, they will be decomposed to release SO_2 due to their thermal unstability at the conditions of FCC process, which means that the De-SO_x activity is very low, this also disagrees with our results of the De-SO_2 activity measurements [31]. Therefore, we deduce that it is impossible that only the individual Mg^{2+} (Fe^{3+} or Al^{3+}) ion is responsible for the sulfate formation. It is likely a mixed metal sulfate.

Iron ions play an essential role in the above cycle. First, iron ions directly involved in the formation of the mixed sulfate, since they can easily be reduced by hydrogen, the sulfate formed, therefore, can effectively be decomposed. Also because of the existence of iron ions, the mixed sulfate is still stable at 973 K comparing to aluminum sulfate or iron sulfate, which diminishes the inverse decomposition.

Second, when iron ions are introduced into the structure of the magnesium–alumina spinel catalyst, the activity of SO_2 adsorption is enhanced [12–15]. This can be explained by two ways: on one hand, Al^{3+} partially substituted by Fe^{3+} can give rise to a crystal strain effect in the crystalline structure of the $MgAl_{2-x}Fe_xO_4$ catalysts, which results in the lattice oxygen being more active than the lattice oxygen in the magnesium–alumina spinel catalyst [32]. Lattice oxygen is the adsorption center of SO_2, hence, SO_2 can easily adsorb on these more active sites. On the other hand, at the end of each reduction cycle, some additional oxygen vacancies are produced, therefore, more oxygen molecules can be adsorbed in the following oxidative adsorption half cycle, producing more active reaction species. All these factors are favorable to the formation of sulfate and hence the SO_2 adsorption activity is improved.

4. Conclusions

(1) The results of the electrical conductivity measurement show that on the surface of the

catalyst the adsorption sites for O_2 are oxygen vacancies. The sites for SO_2 adsorption and reaction are the surface lattice oxygen ions. During the SO_2 adsorption and reaction procedure, some conduction electrons were generated; in the case of oxygen adsorption, however, adsorbed oxygen species consumed the electrons trapped at the oxygen vacancies.

(2) Three bands, respectively located at 850, 910 and 1340 cm^{-1} in the in situ IR spectra, were observed when SO_2 was adsorbed in oxygen free mixture, which are ascribed to the weakly adsorbed SO_2 and the surface sulfite-like species. In the case of SO_2 oxidative adsorption, sulfate ions were formed.

(3) In the reduction half cycle, most of the sulfates, formed in the oxidative adsorption half cycle, were decomposed into a large amount of H_2S together with some SO_2.

(4) Different iron species, Fe^{3+}, $Fe^{2.5+}$, Fe^{2+} and α-Fe^0, were identified in the sulfated and reduced sample in the half cycle of the reduction. When the unsulfated sample was reduced by hydrogen, Fe_3O_4 phase was not found.

(5) A mechanism for SO_2 oxidative adsorption and the reduction decomposition of the sulfate is proposed. Iron ions and another ion are involved in the formation of mixed sulfate, which simultaneously improves the activity of SO_2 oxidative adsorption and the reducibility of the mixed sulfate.

Acknowledgements

The authors are grateful to the National Natural Science Foundation of China and China Jinling Petrochemical Cooperation for their financial support. Discussions with Dr. E. Ley-Koo and Dr. R. Gómez are gratefully acknowledged.

References

[1] J.I. Vernon, Report IEACR/11, IEA Coal Research, London, UK, 1989.
[2] J.I. Vernon, Report IEACR/11, IEA Coal Research, London, UK, 1989.
[3] C.M. Zhang, X.Y. Lin, Environ. Prot. Sci. (China) 20 (1994) 71.
[4] J.W. Byrne, B.K. Spernello, Oil Gas J. 15 (1982) 101.
[5] D.P. MxArthur, H.D. Simpson, K. Baron, Oil Gas J. (1983) 70.
[6] R.J. Bertolacini, USP, 4 381 991, 1986.
[7] P.S. Lowell, K. Schwizgebel, T.B. Pasons, K.J. Sladek, Ind. Eng. Chem. Prod. Des. Dev. 10 (1971) 384.
[8] A.A. Bhattachryya, G.M. Woltermann, Ind. Eng. Chem. Res. 27 (1988) 1357.
[9] E.J. Demmel, 1993 NPPA Annual Meeting, San Antonio, TX, March 21–23, 1993.
[10] J.C. Summers, Environ. Sci. Technol. 13 (1979) 321.
[11] A.A. Bhattachryya, G.M. Woltermann, J.A. Yoo, W.F. Cornier, ACS Meeting, Aug. 30.–Sept. 4, 1987.
[12] J.S. Yoo, A.A. Bhattachryya, C.A. Radlowski, Ind. Eng. Chem. Res. 31 (1992) 1252.
[13] J.S. Yoo, A.A. Bhattachryya, C.A. Radlowski, Appl. Catal. B: Environmental 1 (1992) 169.
[14] J.A. Wang, O. Novaro, C.L. Li, 15th Meeting of the North America Catalysis Society, Chicago, May 18–22, 1997, p. 65.
[15] F.T. Clark, M.C. Springman, D. Wiñncox, I.E. Wachs, J. Catal. 139 (1993) 1.
[16] A. Corma, A.E. Palomares, F. Rey, Appl. Catal. B: Environmental 4 (1994) 29.
[17] M.E. Baldwin, J. Chem. Soc. (1961) 3123.
[18] R.A. Mateus, J.M. Fresco, J. Chem. Phys. 27 (1957) 564.
[19] K.C. Schreiber, Anal. Chem. 21 (1949) 1168.
[20] T. Yamaguechi, T. Jin, K. Tanabe, J. Phys. Chem. 90 (1986) 3148.
[21] S.W. Nam, G.R. Gavalas, Appl. Catal. 74 (1991) 53.
[22] S.W. Nam, G.R. Gavalas, Appl. Catal. 55 (1989) 193.
[23] J.A. Wang, L.F. Chen, C.L. Li, React. Kinet. Catal. Lett., in press.
[24] C.P. Bean, J.D. Livingaston, J. Appl. Phys. 30 (1959) 120.
[25] M.C. Hobson, H.M. Gager, J. Catal. 16 (1970) 254.
[26] J.A. Wang, L.F. Chen, C.L. Li, J. Mater. Sci., in press.
[27] T. Urakawa, T. Nakazawa, J. Mater. Sci. Lett. 15 (1996) 1237.
[28] I. Mitov, S. Asenov, React. Kinet. Catal. Lett. 50 (1993) 145.
[29] R.Z. Ma, Mössbauer Spectroscopy, Bejing Institute of the Iron and Steel, Beijing, 1982.
[30] F. Habashi, S.A. Mikhal, J. Can. Chem. 54 (1976) 3646.
[31] J.A. Wang, C.L. Li, Mater. Lett. 32 (1997) 223.
[32] J.A. Wang, PhD Dissertation, East China University of Science and Technology, Shanghai, China, 1995, p. 66.